

High Intensity Focused Ultrasound for Cancer Treatment: Current Agenda and the Latest Technology Trends

Jongbum Seo*

*Department of Biomedical Engineering, Yonsei University, Wonju 220-710

(Received April 9, 2010; accepted June 9, 2010)

Abstract

High Intensity Focused Ultrasound (HIFU) is a noninvasive surgical method mainly targeting deeply located cancer tissue. Ultrasound is generated from an externally located transducer and the beam is focused at the target volume, so that selective damage can be achieved without harm to overlying or surrounding tissues. The mechanism for cell killing can be combination of thermal and cavitation damage. Although cavitation can be an effective means of tissue destruction, the possibility of massive hemorrhage and the unpredictable nature of cavitation events prevent clinical application of cavitation. Hence, thermal damage has been a main focus related to HIFU research. 2D phased array transducer systems allow electronic scanning of focus, multi-foci, and anti-focus with multi-foci, so that HIFU becomes more applicable in clinical use. Currently, lack of noninvasive monitoring means of HIFU is the main factor to limit clinical applications, but development in MRI and Ultrasound Imaging techniques may be able to provide solutions to overcome this problem. With the development of advanced focusing algorithm and monitoring means, complete noninvasive surgery is expected to be implemented in the near future.

Keywords: High Intensity Focused Ultrasound (HIFU), Focused Ultrasound Surgery, Thermal ablation, Temperature monitoring

1. Introduction

Ultrasound imaging is one of the most widely used medical diagnostic imaging modality in practice. Low energy ultrasound sound is generated from the imaging transducer and the reflected wave is processed to create anatomic imaging of human body. The energy level used in ultrasound imaging is sufficiently low that no adverse biological effect is induced within tissue. According to the FDA regulation for ultrasound imaging system, the spatial peak temporal average intensity (I_{SPTA}) should be

less than 720 mW/cm^2 [1]. However, ultrasound can also be used as a therapeutic means by increasing the energy level properly. High intensity focused ultrasound (HIFU), which is also known as focused ultrasound surgery (FUS), is one the example of high energy ultrasound for the therapeutic purpose [2-7].

HIFU was first implemented by the group in University of Illinois in the 1950s [4-6]. The first system adopted geometrically aligned small number of quartzes to form a focus in depth. The system could successfully induce tissue damage at the focal zone without adverse effect on intervening tissue, but it has never been used in clinically. It was because the original target application of the first

Corresponding author: Jongbum Seo (jongbums@yonsei.ac.kr)
Department of Biomedical Engineering, Yonsei University, Wonju 220-710

HIFU system was Parkinson's disease and chemical treatment was developed soon after the first HIFU system implementation. HIFU was rediscovered as a cancer treatment means in the 1970s. At the earlier stage, temperature of target tissue volume is generally raised up to 43 °C for an extended time (1 hour) using moderate energy level ultrasound in order to increase chemo/radio therapy effects, and this method was known as hyperthermia [8–11]. Later, HIFU was researched to ablate cancer tissue with ultrasound energy alone. Unlike hyperthermia, HIFU induces localized temperature increase more than 60 °C and causes tissue necrosis directly [2], [3], [12–14]. Figure 1 shows the principle of HIFU technique. As can be seen in Figure 1, large volume of cancer can be treated with scanning of a single focus.

The biggest advantage of HIFU in cancer treatment is selectivity and non-toxicity. HIFU can create as small volume damage as 10 mm × 1 mm × 1mm in deeply located tissue without any collateral damage. Additionally, HIFU does not require incision even though HIFU is surgical procedure. In other words, HIFU is completely noninvasive, so that medical complications such as infections and blood loss can be prevented. This noninvasive surgical method also reduces recovery time and many procedures could be done on an outpatient basis. Hence, HIFU can significantly reduce the cost of cancer treatment and HIFU can

greatly improve the life quality of patients .

Although HIFU has great potential as a cancer treatment means, there are number of critical issues to be overcome in HIFU. First, HIFU generally requires long surgery time due to small focus size. Since only small area can be treated with convention scanning and sufficient cooling time has to be provided to avoid collateral damage, treatment duration should be elongated accordingly [15]. Second, monitoring methods needs to be developed to observe treatment results during the procedure. Even though temperature can be a critical indicator in HIFU, noninvasive temperature monitoring is difficult to achieve with conventional medical imaging systems. Third, aberration of focus due to bone tissue needs to be corrected. Since major organs are protected by bone tissue, large acoustic window cannot be obtained easily. Hence, the distortion of focus due to inhomogeneous intervening tissue needs to be properly compensated.

The current technical status of HIFU related to the critical issues is reviewed in this article. The remainder of this paper is divided into five sections. Bio-effect of HIFU and its mechanisms are introduced briefly in section two. Section three explains the phased array system and technical advances in multiple foci in order to reduce surgery duration. Section four covers monitoring methods of HIFU including MRI and Ultrasound thermometry. Section five presents acoustic window agenda to achieve the aberration correction through bone tissue and summary is presented in the final section.

II. Bio-effects of HIFU

Tissue damage caused by HIFU is mainly related to temperature change and cavitation. If temperature is increased for enough duration, necrosis in tissue can be observed [2],[3],[7],[13]. On the other hand, cavitation alone can induce cell rupture without significant macroscopic temperature increases [16–19].

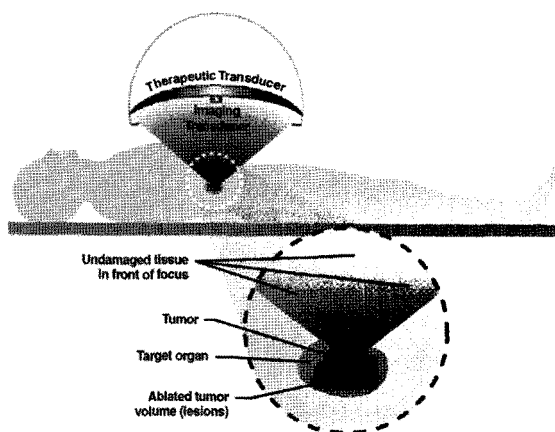


Fig. 1. Principal of HIFU (adapted from reference [14]).

Figure 2A shows a macroscopic picture of coagulation necrosis in the canine kidney. If temperature increased more than 60 °C, cell death generally occurs within a 1 second in most of tissues. Tissue necrosis can be confirmed by pyknotic nuclei, tubular dilation from histology slide, as can be seen in Figure 2B. Pit can be also formed during HIFU procedure even for pure thermal ablation. It is due to that the probability of cavitation increases drastically as temperature increases at the focus.

Figure 3 shows an example of cavitation damage in porcine liver. Unlike thermal damage, pit is formed at the center and sharper boundary of damage zone can be observed around the pit. Generally, large collection of bubbles can be easily detected in ultrasound imaging during cavitation damage. In addition, if the treated area is sonicated with proper intensity, the backscattering coefficient become sufficiently small due to the collapse of the formed bubbles after pulverization of tissue and it can be visualized in ultrasound imaging as shown in Figure 4 [17], [18]. Even though cavitationally induced damage has advantages such as easy observation with ultrasound imaging and possibly clearer damage

boundary, FDA is strongly against cavitation in HIFU procedure due to internal bleeding and unpredictable nature of cavitation [21].

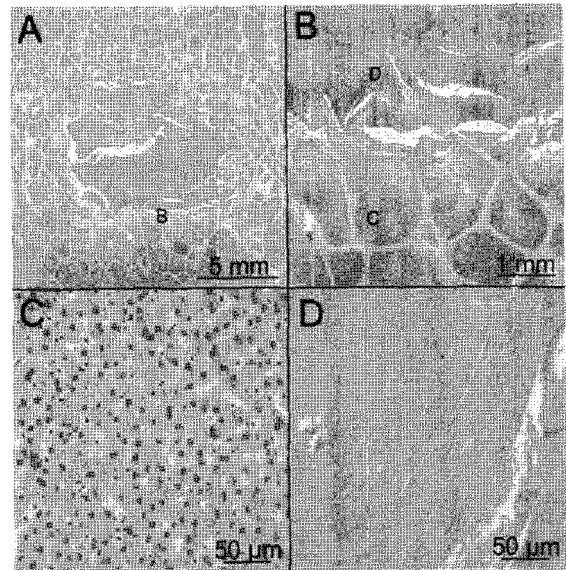


Fig. 3. Selected histology (H & E stain) from a lesion created through histotripsy. Low magnification image A shows a square region of disruption. Magnified image B of the location marked on image A shows the border of the lesion with a transition zone of partial disruption about 1 mm in width. Further magnification in images C and D in which marked areas show normal-appearing hepatocytes in the area outside the disrupted region (C) and a complete loss of cellular structure within the disrupted zone (D) (adapted from reference [17]).

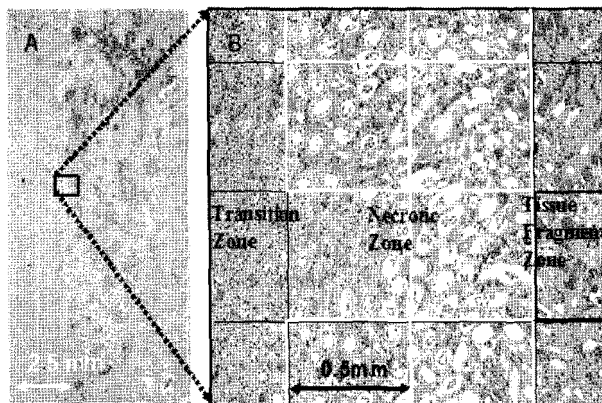


Fig. 2. Microscopic view of overall damage (A). The zone in the center of the field is characterized by multiple areas of hemorrhage and architectural disruption of the necrotic parenchyma. This field is largely occupied by dilated, necrotic tubules in the middle as shown in B, the magnified view of A. At the left is an ill-defined zone of largely viable tubules, mixed with occasional cells showing pyknotic nuclei. On the right side is a portion of the zone of tissue disruption. (adapted from reference [20]).

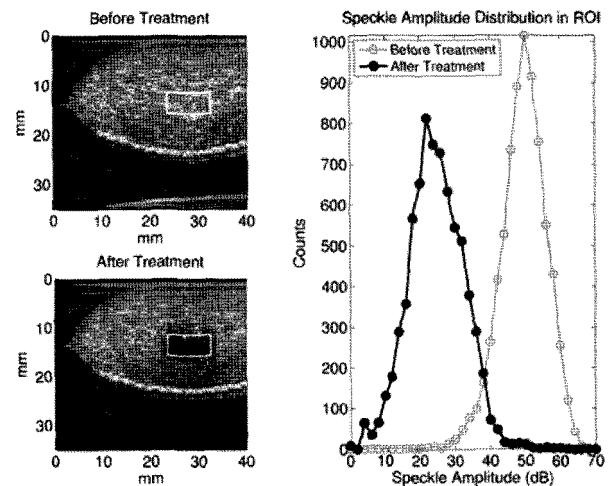


Fig. 4. Sample B-scan images before and after treatment (left) and corresponding histograms (right) for the treatment area ROI indicated by the rectangle. B-scan images are displayed on a 60-dB dynamic range scale (adapted from reference [17]).

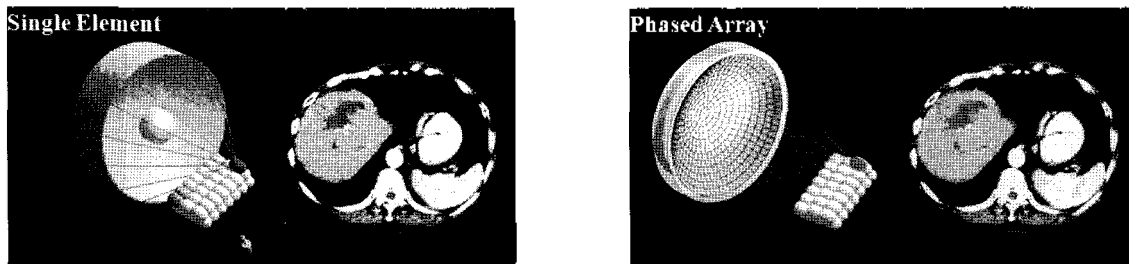


Fig. 5. Mechanical steering with single element transducer (left) and electronic scanning with phased array transducer (right).

III. Phased Array System

In the early stage of HIFU development, mechanical scanning of a single element transducer was adopted to cover large treatment area. Although mechanical scanning can be equally effective, this procedure requires precision position control system and longer surgery duration. As in ultrasound imaging, electronic scanning has replaced mechanical scanning thanks to the development of 2D phased array [20–24]. The difference of two scanning was visualized in Figure 5. Since electronic scanning speed is on the order of microseconds, mechanical scanning is only available at the low end products. Currently, HIFU transducers are generally composed of 200–500 element whose size is on the order of 10 mm^2 and are operated around at 1 MHz. The elements are located semi random pattern to avoid systematic grating lobes during electronic scanning. Figure 6 shows an example of 2D phased array transducer with 513 elements [26].

As mentioned in the introduction, a single focus of therapeutic transducer is on the order of $10 \text{ mm} \times 1 \text{ mm} \times 1 \text{ mm}$. Hence, hundreds of focal points are

required to cover large tumor volume and surgery duration elongated even with fast electronic scanning. In order to overcome this problem, multi-foci using phased array was proposed and implemented in 1990s as can be seen in Figure 7 [25]. Although multi-foci appeared to be effective at first, multi-foci method does not have any advantage over a fast electronic scanning. It is due to that electronic scanning speed is on the order of microseconds and temperature increase late in tissue is on the order of milliseconds [12], [26]. Therefore, two methods shares almost identical results in most of cases [12].

In the recent research, a new approach to utilize phased array system known as anti-foci, which is defined as a zero amplitude pressure point due to destructive diffraction, was proposed [26]. Unlike simple multi-foci which utilize multiple focal points at the same time, anti-foci method utilizes combination of foci and anti-foci at the same time. The biggest advantage of anti-foci method is that it can provide active protection at the random position during HIFU procedure. This active protections are greatly useful for important tissues such as nerve, organ wall, and major vessels. In addition, this

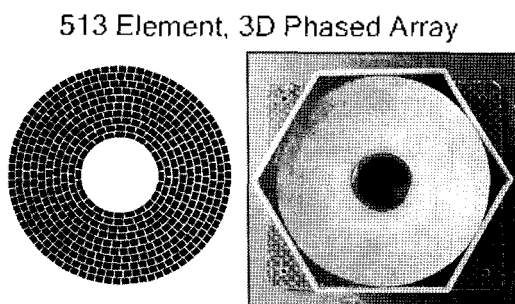


Fig. 6. Typical therapeutic phased array transducer. 513 element.

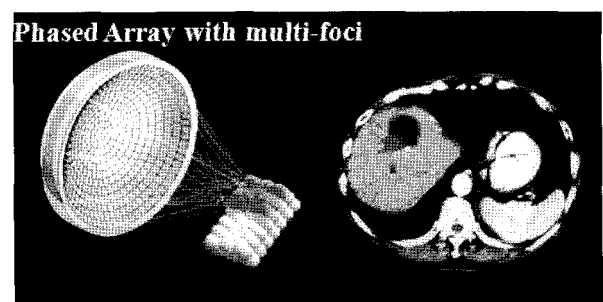


Fig. 7. Multi-foci to cover large volume simultaneous.

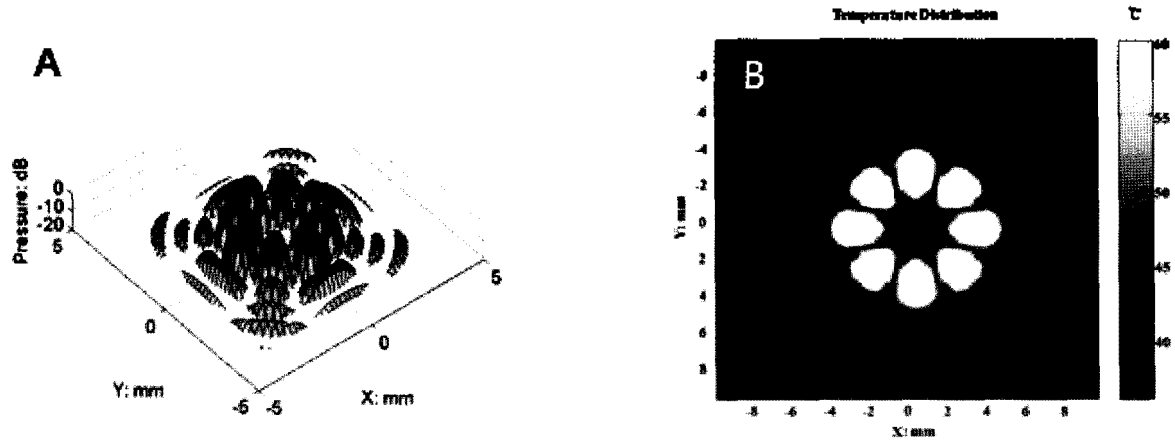


Fig. 8. An application example of anti-foci with multi-foci. A shows pressure field pattern at the central plane where 4 foci and 1 anti-focus is applied. B shows the expected temperature distribution at the central plane when pressure field of 8-A is applied for 3 seconds with maximum pressure amplitude of 6 MPa.

algorithm can greatly reduce surgery duration since no cooling time duration is required during HIFU procedure unlike multi-foci and a fast scanning of single focus.

IV. HIFU monitoring (thermometry)

Noninvasive monitoring is the most critical problem in HIFU. Generally, thermally induced tissue cannot be immediately distinguished from medical imaging unless macroscopic structural change occurs. Hence, the treatment area can be successfully confirmed from MR imaging only after 1 week or so. However, real time monitoring means of HIFU procedure should be provided for the successful treatment.

Thermal damage caused in HIFU procedure can generally be predicted by thermal dose. It is defined as

$$D(x, y, z) = \int_0^{t_f} R^{T(x, y, z; t) - T_{ref}} dt \quad (1)$$

where $T(x, y, z; t)$ is tissue temperature and t_f is the duration of the temperature elevation [15]. R is generally given as in equation (2).

$$R = \begin{cases} 4, & T(t) \leq 43^\circ\text{C} \\ 2, & T(t) > 43^\circ\text{C} \end{cases} \quad (2)$$

Generally, 50–250 equivalent minutes at 43°C is the required thermal dose for irreversible tissue damage [15]. Hence, if the complete temperature profile can be obtained, thermal dose can be determined. Among medical imaging modalities, ultrasound imaging and MRI have been proposed as the monitoring temperature change in tissue.

The basic principle of MRI thermometry is detecting shift of proton resonance frequency as temperature increase ($-0.01 \text{ ppm}/^\circ\text{C}$) [27]–[32]. For example, a 1.5 T imaging system, with a Larmor frequency of 63.9 MHz for water protons, exhibits a temperature dependent frequency shift of $0.639 \text{ Hz}/^\circ\text{C}$. This relationship can be mathematically formulated as in equation (3).

$$\Delta\Phi = TE \cdot \Delta f \cdot 2\pi = TE \cdot \beta \cdot \Delta T \cdot \gamma \cdot B_0 \cdot 2\pi \quad (3)$$

where Φ is the phase of the proton spin magnetization, TE is the time of echo formation, β is the shift constant, ΔT is the temperature elevation, γ is the gyromagnetic ratio of proton, and B_0 is the main magnetic field flux density. The phase change is linearly dependent on temperature change even beyond the tissue necrosis as can be seen in Figure 9. MRI thermometry generally provides the spatial resolution of 1 mm and the temperature resolution

of 1°C.

Thermometry based on ultrasound imaging using the temperature dependent speed of sound (SOS) [33–39]. As can be seen in figure 10, SOS increases in pure water if temperature increases. Ultrasound imaging appears contracted with small temperature increase since wave travels slightly faster. This changes can be quantified by traveling time as can be seen in equation (4).

$$\Delta t_c(z) = 2 \int_0^z \left[\frac{1}{c(\xi, T(\xi))} - \frac{1}{c(\xi, T_0)} \right] d\xi \quad (4)$$

where t_c is traveling time of sound wave, c is temperature dependent SOS, T is temperature, T_0 is initial temperature, and ξ is depth. In equation (4), thermal expansion was ignored since thermal expansion effect is one order smaller than SOS change effect on ultrasound imaging. Assuming SOS is linearly dependent on temperature, local SOS can be approximated as equation (5).

$$c(z, T(z)) = c_0(z)(1 + \epsilon(z) \cdot \Delta T(z)) \quad (5)$$

where $\epsilon(z) = \frac{1}{c_0(z)} \cdot \left. \frac{\partial c(a, T)}{\partial T} \right|_{T=T_0}$, and $c_0(z) = c(z, T_0)$.

By differentiating equation (4) with respect to z and combining with equation (5), we get:

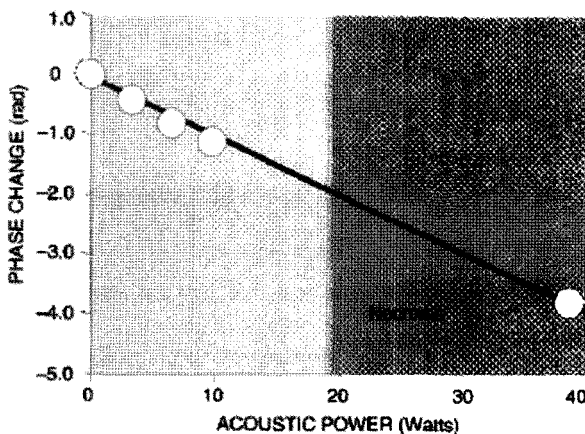


Fig. 9. Phase change due to proton resonance frequency shift is a linear function of applied acoustic power even beyond the level of tissue necrosis. (adapted from reference [3])

$$\Delta T(z) = \frac{c_0(z)}{2} \frac{1}{1 - \epsilon(z)} \frac{\partial}{\partial z} (\Delta t_c(z)) \quad (6)$$

Hence, temperature can be estimated by tracking the time shift in ultrasound imaging. Development of speckle tracking algorithm for ultrasound elastography provides excellent means to estimate time shift up to sub-micrometer level. By adopting phase sensitive speckle tracking algorithm, temperature map can be established up to 45 °C level. Unfortunately, the relationship between SOS and temperature is not linear in biological tissue as indicated in Figure 11 [40]. In addition, SOS decreases in fatty tissue as temperature increases. Therefore, temperature map based on SOS could not be successfully obtained from ultrasound imaging up to the target level of 70 °C. Currently, tissue elastic models and lateral thermal expansion model are proposed by number of researchers in ultrasound imaging thermometry as alternatives.

As mentioned above, MR guided HIFU has great advantages over ultrasound imaging guided HIFU such as high resolution 3D imaging and accurate thermometry. However, integration of MR system with HIFU system not only expensive, but also it limits acoustic window. MR system allows only limited opening of patient, so that HIFU transducer needs to be placed bottom most of cases. On the

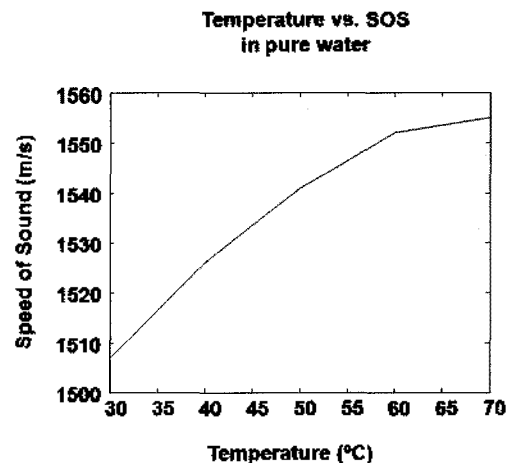


Fig. 10. Temperature dependent speed of sound in pure water. SOS increases almost linearly as temperature increases (reformatted from reference [38]).

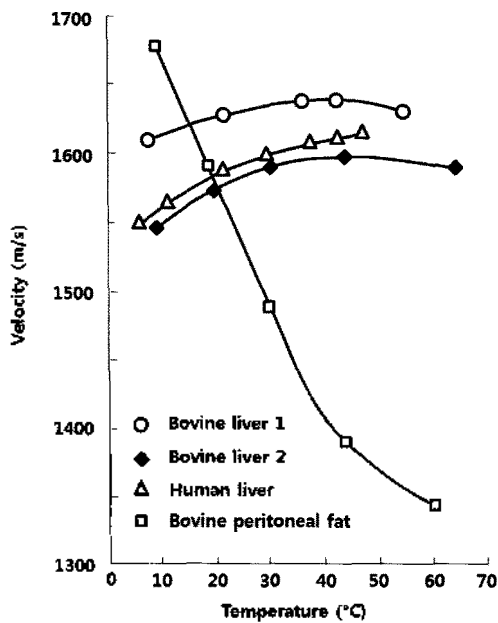


Fig. 11. Temperature dependent speed of sound (reformatted from reference [40]).

Table 1. Acoustic properties of tissue (reformatted from reference [49]).

	Bone	Soft Tissue (Liver)
Acoustic Impedance (MRays)	6.364	1.638
SOS (m/s)	3198	1578
Attenuation Coefficient (dB/MHz · cm)	3.54	0.45

other hand, ultrasound imaging guided HIFU can approach from arbitrary angle. Hence, temperature estimation based on ultrasound imaging is increasingly demanded.

V. Acoustic Window

Unlike ultrasound imaging transducers, the area of an extracorporeal transducer is on the order of 100 cm², in order to generate high intensity ultrasound at the focal spot. Considering larger aperture size of the transducer, large acoustic window needs to be ensured for the adequate treatment on deeply located cancer tissue. Acoustic window problem is especially critical in case of brain and liver, since both organs are protected by bone tissue. Acoustic properties of bone tissue and soft tissue show great

discrepancy as indicated in the table 1. Acoustic impedance mismatch leads to the reflection and scattering of wave, so that great amount of acoustic wave is wasted. In addition, SOS mismatch leads to the aberration on focus formation, so that target point control becomes difficult.

In case of target organ is protected by rib cage such as liver, this problem can be overcome relatively easily with a phased array transducer. Since bone structure is not deformed during HIFU procedure, treatment can be conducted with unblocked elements of phased array transducer as suggested in reference [41].

Even though skull causes high reflection of acoustic wave, high intensity ultrasound still can be transferred through skull to induce thermal damage on brain tumor cells [42]. Instead of reflection, aberration due to inhomogeneous SOS distribution is a more critical problem in HIFU for brain tumor treatment. Since ultrasound beam has to propagate through cranium, its direction can be refracted according to the shape of skull slight. As a result, the focus would not be formed effectively and the possibility of treatment failure increases greatly. In order to overcome this problem, time reverse method was used on the mathematically calculated time delays from target to individual transducer elements based on high resolution 3D CT image [42–48]. Experimental results indicate that this method can be effectively used with MR thermometry. The greatest limit of this method is that movement of patient more than 1 mm can lead to aberration immediately, since wavelength of the ultrasound used in HIFU is approximately 1 mm.

VI. Summary

Thermal necrosis can be successfully induced by HIFU procedure. Development of phased array system and advanced in focusing algorithm of anti-focus with multi-foci suggested that large volume of tissue can be treated at a short period of

time. In addition, the acoustic window problems for HIFU transducers could be overcome with phased array system by adopting time reverse algorithm. Although clinical application of HIFU has been limited due to incomplete monitoring means, this obstacle seems to be resolved with various researches in noninvasive medical imaging system in the near future. This will open the way of implement noninvasive surgery for cancer treatment.

Acknowledgment

This work is the industrial technology innovation program of Ministry of Commerce, Industry & Energy, Republic of Korea.

References

1. FDA, "Information for Manufacturers Seeking Marketing Clearance of Diagnostic Ultrasound Systems and Transducers," 2008.
2. G. ter Haar, "Ultrasound Focal Beam Surgery," *Ultrasound in Med. & Biol.*, vol. 21, pp. 1089–1100, 1995.
3. K. Hynynen, "Focused Ultrasound Surgery Guided by MRI," *Science & Medicine*, vol. 3, pp. 62–71, 1996.
4. W. J. Fry "Action of Ultrasound on Nerve Tissue - a Review," *Symposium on Ultrasound in Biology and Medicine*, 1952
5. W. J. Fry, V. J. Wulpf, D. Tucker, and F. J. Fry, "Physical Factors involved in ultrasound induced changes in living systems: I Identification of Non-Temperature effects," *J. Acoust. Soc. Am.*, vol. 22, pp. 867–876, 1950.
6. W. J. Fry, D. Tucker, F. J. Fry, and V. J. Wulpf, "Physical Factors involved in ultrasound induced changes in living systems: II Amplitude duration relations and the effect of hydrostatic pressure for nerve tissue," *J. Acoust. Soc. Am.*, vol. 23, pp. 364–368, 1951.
7. L. Chen, I. Rivens, G. ter Haar, S. Riddler, C. R. Hill, and J. P. M. Bensted, "Histological Changes in rat liver tumors treated with high-intensity focused ultrasound," *Ultrasound in Med. & Biol.*, vol. 19, pp. 67–74, 1993.
8. J. Overgaard, "Effect of hyperthermia on malignant cells in vivo. A review and a hypothesis," *Cancer*, vol. 39, pp. 2637–2646, 1977.
9. J. H. Kim and E. W. Hahn, "Clinical and Biological Studies of Localized Hyperthermia," *Cancer Res.*, vol. 39, pp. 2258–2261, 1979.
10. C. A. Cain and S. I. Umemura, "Concentric-Ring and Sector-Vortex Phased-Array Applicators for Ultrasound Hyperthermia," *IEEE Trans. Microwave Theory and Techniques*, vol. 5, pp. 542–551, 1986.
11. S. I. Umemura and C. A. Cain, "The Sector-Vortex Phased Array: Acoustic Field Synthesis for Hyperthermia," *IEEE Trans. UFFC*, vol. 36, pp. 249–257, 1989.
12. H. Wan, P. VanBaren, E. S. Ebbini, and C. A. Cain, "Ultrasound Surgery: Comparison of Strategies using Phased array systems," *IEEE Trans. UFFC*, vol. 43, pp. 1085–1097, 1996.
13. L. Poissonnier, J. Y. Chapelon, O. Rouviere, L. Curiel, R. Bouvier, X. Martin, J. M. Dubernard, and A. Gelet, "Control of prostate cancer by transrectal HIFU in 227 patients," *Eur Urol.*, vol. 51, pp. 381–387, 2007.
14. T. J. Dubinsky, C. Cuevas, M. K. Dighe, O. Kolokythas, and J. H. Hwang, "High-Intensity Focused Ultrasound: Current Potential and Oncologic Applications," *AJR.*, vol. 190, pp. 191–199, 2008.
15. W. Hong, "Thermal dose optimization for ultrasound tissue ablation," Ph. D Thesis, Univ. of Michigan, Ann Arbor, 1999.
16. B. C. Tran, J. Seo, T. L. Hall, J. B. Fowlkes, and C. A. Cain, "Microbubble-Enhanced Cavitation for Noninvasive Ultrasound Surgery," *IEEE Trans UFFC*, vol. 50, pp. 1296–1304, 2003.
17. T. L. Hall, J. B. Fowlkes, and C. A. Cain, "A real-time measure of cavitation induced tissue disruption by ultrasound imaging backscatter reduction," *IEEE Trans UFFC*, vol. 54, pp. 569–575, 2007.
18. J. E. Parsons, C. A. Cain, G. D. Abrams, and J. B. Fowlkes, "Spatial variability in acoustic backscatter as an indicator of tissue homogenate production in pulsed cavitation ultrasound therapy," *IEEE Trans UFFC*, vol. 54, pp. 576–590, 2007.
19. A. M. Lake, T. L. Hall, K. Kieran, J. B. Fowlkes, C. A. Cain, and W. W. Roberts, "Histotripsy: A minimally invasive technology for prostate tissue ablation in an in-vivo canine model," *Urology*, vol. 72, pp. 682–686, 2008.
20. J. Seo, B. C. Tran, T. L. Hall, J. B. Fowlkes, G. D. Abrams, M. O'Donnell, and C. A. Cain, "Evaluation of ultrasound tissue damage based on changes in image echogenicity in canine kidney," *IEEE Trans. UFFC*, vol. 52, pp. 1111–1120, 2005.
21. G. R. Harris, "FDA regulation of clinical high intensity focused ultrasound (HIFU) devices," *EMBC*, pp. 145–148, 2009.
22. X. Fan and K. Hynynen, "A study of various parameters of spherically curved phased arrays for noninvasive ultrasound surgery," *Phys. Med. Biol.*, vol. 41, pp. 591–608, 1996.
23. E. S. Ebbini, S. I. Umemura, M. Ibbini, and C. A. Cain, "A Cylindrical-section Ultrasound Phased-Array Applicator for Hyperthermia Cancer Therapy," *IEEE Trans. UFFC*, vol. 35, pp. 561–572, 1988.
24. D. R. Daum and K. Hynynen, "A 256-element ultrasonic phased array system for the treatment of large volumes of deep seated tissue," *IEEE Trans. UFFC*, vol. 46, pp. 1254–1268, 1999.
25. E. S. Ebbini and C. A. Cain, "Multiple-Focus Ultrasound Phased-Array Pattern Synthesis: Optimal Driving-Signal Distributions for Hyperthermia," *IEEE Trans. UFFC*, vol. 36, pp. 540–548, 1989.
26. J. Seo and J. Lee, "Anti-foci for focused ultrasound," *Int. J. Hyperther.*, vol. 25, pp. 566–580, 2009.
27. Y. Wang, J. W. Hunt, and F. S. Foster, "Tissue Ultrasound Absorption Measurement with MRI Calorimetry," *IEEE Trans. UFFC*, vol. 46, pp. 1192–1200, 1999.
28. N. Vykhodtseva, V. Sorrentino, F. A. Jolesz, R. T. Bronson, and K. Hynynen, "MRI Detection of the Thermal Effects of Focused Ultrasound on the Brain," *Ultrasound in Med. & Biol.*, vol. 26, pp. 871–880, 2000.

29. K. Hynynen, A. Chung, T. Fjeld, M. Buchanan, D. Daum, V. Colucci, P. Lopath, and F. Jolesz, "Feasibility of Using Ultrasound Phased Arrays for MRI Monitored Noninvasive Surgery," *IEEE Trans. UFFC*, vol. 43, pp. 1043–1052, 1996.
30. W. C. Connor and K. Hynynen, "Patterns of thermal deposition in the skull during transcranial focused ultrasound surgery," *IEEE Trans. Biomed. Eng.*, vol. 10, pp. 1693–1706, 2004.
31. X. Yin, L. M. Epstein, and K. Hynynen, "Noninvasive transesophageal cardiac thermal ablation using a 2-D focused, ultrasound phased array: a simulation study," *IEEE Trans. UFFC*, vol. 53, pp. 1138–1149, 2006.
32. J. Palussiere, R. Salomir, B. Le Bail, R. Fawaz, B. Guesnon, N. Grenier, and C. Moonen, "Feasibility of MR-guided focused ultrasound with real-time temperature mapping and continuous sonication for ablation of VX2 carcinoma in rabbit thigh," *Magn. Reson. Med.*, vol. 49, pp. 89–98, 2003.
33. R. Seip and E. S. Ebbini, "Noninvasive estimation of tissue temperature response to heating fields using diagnostic ultrasound," *IEEE Trans. Biomed. Eng.*, vol. 42, pp. 828–839, 1995.
34. R. Seip, P. VanBaren, C. A. Cain, and E. S. Ebbini, "Noninvasive real-time multipoint temperature control for ultrasound phased array treatments," *IEEE Trans. UFFC*, vol. 43, pp. 1063–1073, 1996.
35. C. Simon, P. VanBaren, and E. S. Ebbini, "Two-dimensional temperature estimation using diagnostic ultrasound," *IEEE Trans. UFFC*, vol. 45, pp. 1088–1099, 1998.
36. R. Maass-Moreno, "Noninvasive temperature estimation in tissue via ultrasound echo-shifts Part I. Analytical model," *J. Acoust. Soc. Am.*, vol. 100, pp. 2514–2521, 1996.
37. R. Maass-Moreno, "Noninvasive temperature estimation in tissue via ultrasound echo-shifts Part II. In vitro study," *J. Acoust. Soc. Am.*, vol. 100, pp. 2522–2530, 1996.
38. L. E. Kinsler, A. R. Rey, A. B. Coppens AB, and J. V. Sanders, *Fundamentals of acoustics 4th ed.*, John Wiley & Sons, 2000.
39. M. Pernol, M. Tanter, J. Bercoff, K. R. Waters, and M. Fink, "Temperature estimation using ultrasonic spatial compound imaging," *IEEE Trans. UFFC*, vol. 51, pp. 606–615, 2004.
40. J. C. Bamber and C. R. Hill, "Ultrasonic attenuation and propagation speed in mammalian tissues as a function of temperature," *Ultrasound Med. Biol.*, vol. 5, pp. 149–157, 1979.
41. R. J. McGough, M. L. Kessler, E. S. Ebbini, and C. A. Cain, "Treatment Planning for Hyperthermia with ultrasound phased arrays," *IEEE Trans. UFFC*, vol. 43, pp. 1074–1084, 1996.
42. J. F. Aubry, M. Tanter, M. Pernol, J. L. Thomas, and M. Fink, "Experimental demonstration of noninvasive transskull adaptive focusing based on prior computed tomography scans," *J. Acoust. Soc. Am.*, vol. 113, pp. 84–93, 2003.
43. K. Hynynen, G. T. Clement, N. McDannold, N. Vykhodtseva, R. King, P. J. White, S. Vitek, and F. A. Jolesz, "A 500 element ultrasound phased array system for noninvasive focal surgery of the brain — a rabbit study with ex vivo human skulls," *Magnetic Resonance Imaging*, vol. 52, pp. 100–107, 2004.
44. G. T. Clement, P. J. White, and K. Hynynen, "Enhanced ultrasound transmission through the human skull using shear mode conversion," *J. Acoust. Soc. Am.*, vol. 115, pp. 1356–1364, 2004.
45. G. T. Clement, P. J. White, R. L. King, N. McDannold, and K. Hynynen, "A magnetic resonance imaging-compatible, large scale array for trans-skull ultrasound surgery and therapy," *Journal of Ultrasound in Medicine*, vol. 24, pp. 1117–1125, 2005.
46. T. Huttunen, M. Malinen, J. P. Kaipio, P. J. White, and K. Hynynen, "A full-wave Helmholtz model for continuous-wave ultrasound transmission," *IEEE Trans. UFFC*, vol. 52, pp. 397–409, 2005.
47. P. J. White, G. T. Clement, and K. Hynynen, "Transcranial ultrasound focus reconstruction with phase and amplitude correction," *IEEE Trans. UFFC*, vol. 52, pp. 1518–1522, 2005.
48. P. J. White, G. T. Clement, and K. Hynynen, "Local frequency dependence in transcranial ultrasound transmission," *Physics in Medicine and Biology*, vol. 51, pp. 2293–2305, 2006.
49. T. L. Szabo, *Diagnostic ultrasound imaging: Inside out*, Elsevier Academic, 2004.

(Profile)

• Jongbum Seo

Present: Assistant Professor in the Department of Biomedical Engineering, Yonsei University, Wonju, Korea